

Sea Level Changes Induced by Local winds on the West Coast of India

Prakash Mehra^{1#}, Michael N. Tsimplis², R.G. Prabhudesai¹, Antony Joseph¹, Andrew G. P. Shaw², Y.K. Somayajulu¹ and Paolo Cipollini²

1 National Institute of Oceanography, Goa, India

2 National Oceanography Centre, Southampton, UK

[Corresponding author: pmehra@nio.org]

Abstract

The contribution of atmospheric pressure and wind to sea level variability at Goa (West coast of India) for the period 2007-2008 is investigated. Sea level data from a tide gauge are compared with measured local surface meteorological as well as oceanographic data. Multilinear regression analysis is used to resolve the dependence of sea level on various forcing parameters. The multilinear regression analysis performed over ~two years data shows that the local surface meteorological data and water temperature accounts the sea level variability only up to 6%. The accounted sea level variability increases to 25%, when the local wind and the surface currents obtained from satellite altimetry in the near vicinity of the study area are incorporated in the regression analysis. The contribution of local wind increases substantially, when the regression is performed over two month duration and it is variable within the year. During the summer monsoon season (May-September), the sea level variability attributable to wind is up to 47% (75%) respectively for 2007(2008); however it reduces to less than 20% during the winter monsoon (November-February) season. A significant part of the variability observed in sea level remains unaccounted for and is attributed to remote forcing.

Keywords Sea level variability · Altimetry · West coast of India · Surface meteorological forcing · Remote forcing · Multilinear regression · Correlation

1 Introduction

Sea level variability poses significant risks to coastal areas, which primarily results from oceanographic, meteorological and hydrological forcing (Tsimplis and Woodworth, 1994). In addition, tidal constituents have contributions at, monthly fortnightly, seasonal and longer periods. However, their contribution is lower than that of the aforementioned parameters at monthly to interannual scales (Shankar, 2000). Understanding and modeling sea level variability on the basis of its forcing is crucial for coastal planning and protection as well as for forecasting the impacts of climate change that may have on particular locations.

In many parts of the open ocean, knowledge of sea level variability is available. However, at the coastal regions of developing states in Africa (Woodworth et al., 2007) as well as the southern coasts of Asia, and in particular the Indian subcontinent, research has not progressed as fast. This is partly due to the fact that the tide-gauge and meteorological networks have not been developed adequately yet for various reasons. Even where data have been collected for some years, these data have not been fully utilized to provide the necessary information required (Shankar, 2000; Srinivas et al., 2005a & b). However, as the significance of sea level monitoring and the impacts of sea level rise under climate change scenarios become more important, efforts to improve knowledge of sea level variability around the world are intensifying. In India, significant efforts have been undertaken for the establishment of a network of internet enabled real-time reporting sea level and surface meteorological data under a national program on *Observation of sea level and surface meteorological data from coastal locations* (Prabhudesai et al., 2006; 2008). As part of this network, a new tide-gauge and a weather station have been established at Goa.

Goa is located at the west coast of India and is under the influence of the north Indian Ocean (Fig.1). North of $\sim 10^{\circ}\text{S}$, the north Indian Ocean is purely tropical, being confined at its north at around $\sim 25^{\circ}\text{N}$ by the Asian landmass. Its atmospheric circulation is dominated by the seasonally varying monsoon associated with the annual heating and cooling of the Asian continent. The winds generally blow from the southwest during May-September (summer monsoons) and from the Northeast during November-February (winter monsoon); March-April and October being the transition months with weak winds. The winds are stronger during the summer monsoon than during winter monsoon and these reversing monsoonal winds over the north Indian Ocean forces a seasonal reversing circulation in the upper ocean (refer Fig.2, Shankar et al., 2002). The seasonally reversing monsoon currents, open-ocean currents flowing between the Arabian Sea and the Bay of

Bengal, which forms the two wings of north Indian Ocean could be described (refer Wyrcki, 1973; Shankar and Shetye, 1997; Shankar et al., 2002 and references therein) as follow: During winter monsoon (November-February), the East India Coastal Current (EICC) is southward and joins the winter monsoon current (WMC) between 0° to 5° N (around Sri Lanka) which is flowing westward carrying low salinity water from the Bay of Bengal. The WMC divides into two branches in the Arabian Sea. One continues to flow westward, whereas the other turns around the Lakshadweep high (a sea-level high off southwest of India) to flow into the poleward West India Coastal Current (WICC). However, by May (during summer monsoon), the WICC is southward all along the coast; it flows into the eastward flowing summer monsoon current (SMC). The SMC in the Arabian Sea is a continuation of the Somali Current and the coastal current off Oman. It flows eastward and southeastward across the Arabian Sea and around the Lakshadweep low (a sea-level low off southwest of India). The WICC flows southward in the region north of 12° N latitude and the current flowing along the western slope of low, joins the SMC. However, south of 12° N latitude, the WICC flows northward. The low too stretches westward, extending across the southern Arabian Sea by November. The northward (southward) WICC implies coastal downwelling (upwelling) near the study region.

Several studies have been carried out on sea level variability along the west coast of India in various contexts from seasonal to climate change issues (Banse, 1968; Wyrcki, 1971 & 1973; Hasternath and Lamb, 1979; Johannessen et al. 1981; Shetye and Shenoi, 1988; Shankar and Shetye, 1997, 1999, 2001; Srinivas, et al. 2005 a,b; Shetye et al., 2008). The above-mentioned observations suggest that the variations in sea level during the winter (summer) monsoon are linked to the coastal currents around India and to the circulation in the southern Arabian Sea as a whole. Thus, it is expected that the sea level variability would be determined partly by local forcing and partly by sea level variations generated elsewhere (Lighthill, 1969).

In this paper, we examine the ability of local measurements to describe the observed sea level variability at a coastal tide-gauge site at Goa. In particular, the contributions of local atmospheric pressure, wind, atmospheric and water temperature and water density to the observed sea level variations are investigated. The part of sea level variability not explained by the above mentioned forcing factors is likely to be linked to the coastal currents off India or to remote forcing. This is partly expressed through the development of circulation and the currents offshore the location of sea level measurements. In section 2,

we describe the data and the methodology followed; section 3 describes the relationship between sea level and various forcing functions. Section 4, describes the results of analysis for estimation of sea level using barotropical model developed using multilinear regression analysis.

2 Data description

Sea level and surface meteorological parameters are collected at Goa (see Fig.1). Weather data are collected by an automatic weather station (AWS) installed on the building of (~48 m height w.r.t MSL) the National Institute of Oceanography (Mehra et. al., 2005). Sea level is measured using a real-time reporting (Honeywell) pressure and radar tide gauge at Verem near the mouth of the Mandovi estuary (Fig. 1 and Table 1). The horizontal distance between the tide-gauge and the weather station is ~5 km. The observed parameters and the measurement periods covered are shown in Table 1.

Table 1. Summary of the Observations:

Measured Variable	Station	System	Depth/ Height (m)	Data start ^c	Data end ^c
Sea level	Verem ^a	Pressure Gauge	-1.0	1Jan, 2007	31 Dec, 2007
Water temperature	“	CTD	0 to -3	1 Jan, 2007	13 Nov, 2008
Water density	“	Radar Gauge	+4.0	30 March, 2007	13 Nov, 2008
Sea level	“	AWS	+ 48.1	1 Jan, 2008	13 Nov, 2008
Winds, Air temperature, Air pressure, and Relative Humidity	Dona Paula ^b			1Jan, 2007	13 Nov, 2008

^a The sea level, water temperature and water density data are collected from Verem Jetty. For the pressure gauge (Radar gauge) the depth (height) is given with respect to the local chart datum.

^b The surface meteorological parameters are collected from the terrace of NIO building. The AWS height is given with respect to the mean sea level.

^c The local time is Indian Standard Time (IST), which is 05:30 hr ahead of GMT.

Wind, air temperature, air pressure and relative humidity data used in the present study are an hourly record. The AWS samples data every 10 seconds over a window of 10

minute and then averaged to generate an hourly data series. The wind speed measured at a height of ~48 m is estimated at 10 m height [$W_{10}=W_{48}*(10/48)^{0.817}$] with respect to mean sea level and the direction values were used to compute the cross-shore and along-shore components. This decomposition was done using the average angle of orientation of the coast in the vicinity of the anemometer (~-12 degrees w.r.t. North).

The pressure sensor based tide gauge data used in the present study is from January-December 2007 at an hourly interval. The atmospheric pressure corrected sea level obtained from sub-bottom pressure data, is sampled at 2 Hz frequency for five minute duration (600 samples) and then averaged to generate an hourly data time-series. The radar gauge data is used from 1 January, 2008 to 13 November 2008, at an hourly interval. The sea level samples are obtained 1 minute prior to the recoding interval over a 30 second window. The tide-gauge instruments were described in detail by Prabhudesai et. al (2006). The astronomical tide from the measured sea level signal was removed using the TASK-2000 (Bell et al., 1998) tidal analysis and prediction program to obtain the sea level residuals (SLR). The pressure gauge also provided the sensor's (Honeywell, Inc.) compensation temperature as an output and has been used as water temperature (evaluation described in P. Mehra et. al .2008). All the hourly measured sea and atmospheric parameters were subjected to a convolution filter with a Hanning window of 36 data points.

The measurements from the two sea level sensors overlap for a period of three months. The comparison between the residuals from the radar gauge and the pressure gauge during the overlap period from October to December 2007 is shown in fig.2. The tidal residuals for the overlap duration are shown in Fig. 2a. The difference (radar gauge minus pressure gauge) as shown in Fig. 2b has an average of ~-2.0 cm with a standard deviation of ~3.2 cm. The thick line is a 24 hr running average, which remains confined within ± 5 cm. The difference ~-2.0 cm is subtracted from the radar gauge data series to correct the offset between the data from the two systems.

Sea level anomaly (SLA) measured by the Jason-1 satellite along the track-181 (Fig.1a) sampled every 7 km along track with a repeat period of ~9.9156 days. The Jason-1 data were previously corrected for instrumental noise, orbit determination error and geophysical errors, including the loading tide and the inverse barometer effect. Cycles 1 to 252 have been used, so that the time series thus constructed correspond to approximately 7 years of data, from 2002 to 2008. The geostrophic current 'GC' (2007 to 2008) was

estimated as the average of the current obtained from the sea level anomaly gradient from 13° N to 14° N along the satellite track. The estimated currents were interpolated using splines to generate hourly time series, which could then be used along with the other parameters for further analysis. The water density is measured at Verem at a depth of 0-3 m using Seabird, CTD at least two times in a month.

3 Methodology

Sea-level variability can be caused by changes in various forcing functions such as atmospheric pressure, wind stress, ocean circulation and fluctuations in the heat and salt content of the ocean (thermohaline changes).

3.1 Atmospheric pressure

Sea level responds to atmospheric pressure in an inverse way. Increases of local atmospheric pressure imply lowering of local sea level provided that the pressure at the far field remains constant. This inverse barometric correction, η^b is expressed by the relation:

$$\rho g \eta^b = \bar{p}_a - p_a \quad (1)$$

Here, ρ is water density, g is the acceleration of gravity, \bar{p}_a is the spatial average of p_a over the global ocean, and p_a is the atmospheric pressure. With $g \sim 9.8$ m/s, the relationship is approximated by -1 cm/mb of change.

3.2 Wind forcing

In order to examine the wind forcing, a simple model as formulated by Sandstrom (1980), could be used to account for the principal effects of forcing by winds. The main assumptions made were (1) the existence of slow large scale motions and hence $\omega \ll f$,

$\frac{\partial}{\partial y} \ll \frac{\partial}{\partial x}$, (2) shelf width, $L < R_E$, the barotropic radius of deformation, and (3) bottom friction

is not negligible. The principal terms in the momentum balances were then:

$$fv = g \frac{\partial \eta}{\partial x}$$

$$\frac{\partial v}{\partial t} = \frac{\tau_{sy} - \tau_{by}}{\rho h(x)} \quad (2)$$

Where η is sea surface elevation; f is coriolis parameter; $h(x)$ is the depth of water column at x ; τ_{sy} and τ_{by} are the alongshore surface and bottom stress respectively. The geostrophic balance (between the depth-averaged alongshore current ' v ' and offshore pressure gradient) is followed by neglecting terms $\frac{\partial u}{\partial t}$ (' u ' is depth-averaged offshore current), and offshore wind stress. The Coriolis force is neglected in the along-shore momentum balance based on the arguments by Csanady (1974), which follow from assumption-2 above and the overwhelming influence of wind stress in the shallow water.

At low frequencies the alongshore momentum balance is between wind stress forcing and bottom friction with response having negligible time lag for the forcing. The alongshore current has the maximum possible (asymptotic) amplitude

$$v = \left(\frac{|\tau|}{\rho C_D} \right) \quad (3)$$

Where $|\tau|$ is the magnitude of the surface stress due to winds W (wind speed in m/s), taking

$$|\tau| = \rho_{air} C_{D(air)} W^2 \sim 1.5 \times 10^{-3} W^2$$

(Hsu,1974) and $C_D = 1.6 \times 10^{-3}$ (Weatherly,1975), one gets

$$\left(\frac{|\tau|}{\rho C_D} \right)^{1/2} \approx 0.03W \quad (4)$$

Hence, the maximum expected currents are ~3% of the winds. For a constant v along the shelf, the sea surface elevation ' η ', has a constant slope and if assumed that the η vanishes at the shelf edge, then the expected sea level change at the coast is given by

$$\eta = \frac{fL}{g} v \approx 0.03 \frac{WfL}{g} \quad (5)$$

In the present case of study; with shelf length, $L = 1.2 \times 10^5$ m; the Coriolis parameter for the corresponding latitude, $f = 3.7727 \times 10^{-5} \text{ s}^{-1}$; one expects $\eta = 0.013 W$ in meters in this region.

3.3 Local Surface Buoyancy Forcing

The residuals have significant variations because of the seasonal character of oceanic surface buoyancy fluxes (heat and freshwater flux). The time varying component of the residuals η^{sb} as described by Gill and Niiler (1973), can be written as sum of three terms (corrected for effects of atmospheric loading):

$$\eta^{sb} = \eta_s + \eta_{bc} + \frac{1}{g\rho_0} p_b \quad (6)$$

According to their analysis, the surface steric anomaly is defined as:

$$\eta_s = -\frac{1}{\rho_0} \int_{-h}^0 \rho'(z) dz \quad (7)$$

where $\rho'(z,t) = \rho(z,t) - \overline{\rho_0}(z)$ is the time-dependent density anomaly relative to a reference profile. The depth h stands for the base of the seasonal thermocline. The term

$$\eta_{bc} = -\frac{1}{\rho_0} \int_{-H}^{-h} \rho'(z) dz \quad (8)$$

represents the effect of density changes below the seasonal thermocline resulting from the changing currents, predominantly induced by changes in vertical Ekman pumping velocity. The last term represents baroclinic changes induced locally through advection of the T, S field by fluctuating barotropic currents (Fofonoff and Tabata, 1996).

The upper ocean steric height anomaly η_s consist of two terms arising separately from near-surface and freshwater content.

$$\eta_s = \frac{1}{\rho_0} \left(\int_{-h}^0 \frac{\partial \rho}{\partial T} T' dz + \int_{-h}^0 \frac{\partial \rho}{\partial S} S' dz \right) \quad (9)$$

However, previous estimates of Gill and Niiler (1973) suggest, that the second term can be neglected and that the steric height anomaly to first order is determined by the change in the heat content of the seasonal thermocline. This assumption is not true for areas of freshwater outflow or areas of strong evaporation. Joesph et. al., (2002) reported in a study at Marmugao Port, Goa from June 1995 to July 1998, that the surface water

density varied between 1.020-0.996 gcm⁻³. During June-July the density dipped to ~1.000 gcm⁻³ and increased to ~1.020 gcm⁻³ by September and remained at this level till May. Our measurement of water density at Verem also indicate the similar results (Fig. 5f), the water density reduces by ~0.020 (1.020-1000) gcm⁻³ during the summer monsoon. Assuming a depth of 5 m, the sea level residual variation (using equation-7) could be up to ~ 9.8 cm $[(\Delta\rho/\rho) \times h]$.

However, the results of CTD observations in Northern Arabian Sea (during US JGOFS project) by Hyun-Sook Kim et al., (2001) showed that mixed layer depth varied from 75 to 100m. Using the temperature data (~6m depth) from the Arabian Sea project's shipboard ADCP together with a thermal coefficient of $1.6 \times 10^{-4} \text{ }^\circ\text{C}^{-1}$ (Stammer, 1997a), the steric fluctuations obtained ranged from -5 to 4 cm, which were slightly larger than those found in the Indian Ocean south of 20 °N by Stammer (1997b).

Similarly, for the present study, using $h=100\text{m}$, thermal coefficient= $1.6 \times 10^{-4} \text{ }^\circ\text{C}^{-1}$, the temperature anomaly measured ranged from -4.4 to 3.9°C, then the steric fluctuations due to the heat content ranges from -7.07 to 6.3 cm, are slightly higher than the above values and also to the values (-7 to 5 cm) found in the upper 500 m using CTD observations from the six transit along the two US JGOFS transects. The sea level variations estimated by using the equations for the various forcing are as listed below (Also refer Fig. 5):

S. No.	Variable	Estimated sea-level variation (cm)
1	Atmospheric pressure (range = 4 mb)	4
2	Winds (Alongshore peaks up to 5 m/s)	6.5
3	Water density*	9.8
	Estimated sea level variations due to above forcing	20.3
	Measured sea level residual (Fig. 5b)	~30

*The water density reduces by ~0.020 gcm⁻³ during summer monsoon and includes the variations due to water temperature and salinity for a depth of ~5 m.

3.5 Multiple regression analysis

Multilinear regression models of sea level residual as the dependant parameter and with the various atmospheric parameters or their forcing factors above are used to describe sea level variability of the sea level residuals. The model can be described in general as:

$$\eta = B_0 + B_1P + B_2T + B_3V + B_4U + \dots + \varepsilon, \quad (10)$$

where independent variables P, T, U and V are atmospheric pressure, temperature and wind (cross shore and along shore components). How well the model describes the sea level residual is assessed by looking at the percentage of sea level variance explained by the model. The independent parameters were added one at a time. Only where an independent parameter increased the sea level residual variance explained 'var_e', significantly, it was retained in the model.

$$\text{var}_e = \left(1 - \frac{\text{variance}(\text{measured_SLR}) - \text{variance}(\eta)}{\text{variance}(\text{measured_SLR})}\right) \times 100, \quad (11)$$

4 Results

The interannual variability of sea level at the study area is best described on the basis of long term measurements. The mean sea level data from PSMSL station at Marmugao together with nearest and farthest point along the altimeter track are shown in Fig.3 indicating a strong seasonality with low (high) during the summer (winter) monsoon. The seasonal character of the signal varies within this short time series from year to year. The seasonal change includes a sharp sea level rise of about 24 cm from October to November (Banse, 1968). This coincides with the shift of the currents along the west coast of India, when the WICC changes from southward to northward. Similar variations are also seen in the radar altimetry data (red and grey line) which are the monthly-mean sea level anomaly from the nearest (Lat: 14.0°N, Lon: 73.8°E) and farthest (Lat: 9.0°N, Lon: 72.0°E) with respect to the Marmugao along the Jason track are also shown in Fig.3. The correlation coefficient with PSML data for nearest & farthest altimetry data are 0.84 & 0.54 respectively [N=48] at 95% confidence interval with high significance.

We turn now to the analysis of the 2007-2008 data from Goa. The sea level data indicates a strong semi-diurnal tidal signal with a range of ~ 250 cm (Fig. 4a). After the removal of the astronomical tide using TASK-2000 from the measured tides, the residuals range between ± 30 cm (Fig. 4b). The tidal residual variations could be due to winds, coastal currents and thermohaline effects.

The wind speed for the year 2007-2008 is shown in Fig 4c. and the wind direction in Fig. 4d. High wind speed values during June-July ~ 3 ms^{-1} and low winds during January-March ~ 1.2 ms^{-1} are found. After the onset of summer monsoon, the wind is predominantly southwesterly, however one frequently notices periods of breaks in wind direction as shown in Fig. 4d. The winds observed during the summer monsoon are strong, peaks up to 10-12 ms^{-1} and are humid as they originate from sea. During the winter monsoon, the winds are of low magnitude (2-5 ms^{-1}), dry, cool and are of continental origin. These results indicate the conclusions of the Hasternrath and Lamb, (1979) who observed that from November to February the winds in the coastal region off western India are generally southward with monthly mean of ~ 3 ms^{-1} and the winds outside the summer monsoon are weak and of variable direction. The analysis of the winds into along-shore and cross-shore components is shown on Figure 5. The cross-shore winds (Fig. 5c) remain predominantly landward with periods of stronger seaward flow in November and December 2007. Maximum landward values are found in June-July ~ 2.2 ms^{-1} for the year 2007-2008. The along-shore component is in general weaker than the cross shore component. It remains predominantly southward, except during June-August (maximum in July ~ 1 ms^{-1}) and during June (~ 0.7 ms^{-1}) for the year 2007 and 2008 respectively, when the along-shore wind is observed to be northward. It is worth noting that the maximum in the alongshore component each year appears ~ 22 days before the maximum cross shore component.

The atmospheric pressure (Fig. 4e and Fig. 5e) shows seasonal variability with the minimum during June-July 999.1 (1001) mb and maximum during December-January 1007.7 (1006.5) mb for the year 2007 (2008). The range being 8.5 mb. These changes would imply a pressure induced sea level change of 8.5 cm with opposite phase. The seasonal variations in pressure are caused by the differential heat capacity resulting in thermal contrast during summer and winter between the land and the ocean. An inverse relation of winds and atmospheric pressure is evident (Fig. 5 c & e), with a significant correlation of ~ -0.7 .

The relative humidity (Fig. 4h) is high during July-Sept. (81-94 %) and low during November-February (63-71%) consistent with the cross shore wind directions over these periods.

Water temperature (WT) shows a more complicated seasonal variability with a period of consistently higher values in May ~ 32.6 (31.9) °C and a period of consistently lower values in August ~ 27.7 (27.4) °C in 2007(2008), with a range of $\sim 4.7 \pm 0.2$ °C (Fig. 4f). A second period of elevated temperature can be found in November. The air temperature shows a similar pattern to the water temperature (Fig. 4g) but with higher variability in the December – February period.

The measured density from 30 March 2007 (The density values from January to 15 March is assumed to be 1.020 gcm^{-3} (Fig. 5f). The water density fall to $\sim 1.0 \text{ gcm}^{-3}$ by mid June and remains low till September. Joseph *et.al.*, (2002) reported in a study at Marmugao Port, Goa from June 1995 to July 1998, that the surface water density varied between $1.020\text{-}0.996 \text{ gcm}^{-3}$. During June-July the density dipped to $1.000 \pm 0.005 \text{ gcm}^{-3}$ and increased to 1.020 gcm^{-3} by September and remained at this level till May. Then, it sharply declined to $1.000 \pm 0.005 \text{ gcm}^{-3}$ by June. The estimated geostrophic current from the altimetry data is shown in Fig. 5b. Currents appear southward during the summer monsoon. However, during the winter monsoon, the current is northward in agreement with previous published studies. Johannessen *et al.*, (1981) note that in November and December the coastal flow reverses from a narrow & shallow southward coastal current to a 40 km wide jet-like flow along the continental slope off the northwest coast of India. The transport of this current has been estimated to be $7 \times 10^6 \text{ m}^3 \text{ s}^{-1}$ (Shetye and Shenoi, 1998).

The correlation coefficients (R) between the various parameters as shown in fig. 4 and Fig. 5 and the sea level residuals are listed in Table 2. The correlation coefficients for the monthly mean are stated and significance is reported at 95% confidence interval. The monthly mean sea level residuals are not correlated with any of the measured surface meteorological and oceanographic variables. Of course many of the atmospheric parameters are correlated with each other. Atmospheric pressure is significantly correlated with winds, relative humidity and water density. By contrast atmospheric temperature (AT) is correlated only with water temperature and the water density shows correlation with cross-shore winds, atmospheric pressure and relative humidity.

A careful examination of Fig. 5 cannot help in resolving the dominant forcing factors of sea level variability. Most of the parameters discussed include a period in the year, where variability is strong and other quieter periods. However, the tidal residuals provide a different picture. First, variability is present throughout the year. The peaks of some parameters do correlate to sea level peaks. For example the peak in geostrophic current and cross shore winds around day 8th August 2007 is also visible in the sea level data. The same can be said for the cross-shore wind and tidal residuals at around day 24th June 2007 and day 13th June, 2008. However, there are strong sea level signals, for example around day 20th May, 2007 and 5th February 2008 that do not coincide with any similar signal in the atmospheric time series. Note also the dip in sea level around day 20th May 2008 which coincides with the minimum in geostrophic current and possibly with smaller signals in along and cross shore winds. Sandstorm, (1980) observed that phase lag of η to wind increased rapidly for $0.2 < f < 0.5$ cpd. Their estimation indicated that the frictional adjustment time “T” as coined by Csanady (1974) lies in the range of $2 < T < 5$ days.

$$T = h \left(\frac{\rho}{C_D |\tau|} \right)^{\frac{1}{2}}$$

For $h = 100$ m, an estimate for T is $\sim 2 \times 10^6 / W$ s. Thus for $W = 10$ m/s, $T \sim 2$ days. Hence our assumption that the variations in the sea level residual follow winds closely is correct, as the data is averaged for 3 days, using a convolution filter.

The power spectra of the tidal residuals and the atmospheric forcing functions are shown in Fig. 6. Four main frequencies can be identified at 0.083, 0.25, 1 and 2 cpd (i.e. Time period $T=12$ days, 4 days, 1 day and 0.5 day respectively). The data used for spectrum analysis is from 5th May 2007 to 13th November 2008 of hourly data series without use of filter. The spectrum of data series is obtained using the ‘pwelch’ function (confidence limit-95%) from Matlab over the total number of samples $N=13463$ with Hamming window of length-2096 points with a 50% overlap. The lower frequencies are not identified in the spectrum due to the choice of the window (~ 87 days) over which the spectrum analysis is performed. Krishnamurty and Bhalme (1976) also noted oscillation around 11.5 and 4.5 days in pressure of monsoon trough and 11.5 and 3.5 days in Mascarene high. The 24h and 12h peaks in the atmospheric forcing and the tidal residuals may be linked. The harmonic analysis of atmospheric pressure variations (atmospheric tides) for year 2007 shows that semidiurnal ($S2 = 1.4$ mb, $M2= 0.09$ Mb) and diurnal frequency ($S1 = 0.6$ mb, 0.02 mb) are $\sim \pm 2$ mb, which may lead to sea level variations of $\sim \pm 2$ cm. However the main

tidal components are around 24 h and 12 h and therefore the case may be that the signal in the tidal residual spectrum is due to tides.

Regression models

The results of the multilinear regression analysis of various independent parameters on sea level residuals as the dependent parameters are listed in Table 3 and 4. The coefficients are estimated at 95% confidence interval. Various methodologies have been experimented with in order to successfully model the signals.

As a first approach, the regression was performed over the full hourly data from 1 September 2007 to 13 November 2008. In addition to wind components, wind stress was also used as independent parameter. This standard regression technique had very little success as by using the whole period only ~6% of the sea level residual variability could be accounted for (Table. 3a). Only when the geostrophic current was included, the value of variance explained was raised to around 25%. Table. 3b is listed with the estimates of coefficient along with the lower (upper) confidence bound and the R^2 (statistic) ~0.24, for the independent variables AP, U, V and GC.

However, with the inclusion of 'GC' many of the peaks (Fig. 7) for example peak No-4 at day 29th July, 2007 are explained. Similarly, during January-May, 2008 the variability in residuals is better explained. These variations are also visible in geostrophic currents (Fig. 5 a&b) but not in the winds and indicates that these sea level residuals are not caused by local winds.

The contrast between water and atmospheric temperature ($WT - AT = T_{diff}$) is reported to cause a seasonal change in the drag coefficient of air and water (Csanady, 1974), which may vary by as much as by a factor of 2 (Hsu, 1974). Therefore, T_{diff} or WT and water density were also include as an independent parameter along with AP, U, V and GC, a small improvement was found in the variance explained (Table. 3a). The WT data was linearly interpolated for the gaps (Fig. 4f) except from day 21st March to 30th April, 2007.

The residual time series examined indicate significant differences between the summer (winter) monsoon and the other periods. For this reason, we model the data using a multilinear regression in moving non-overlapping windows of two months (~60 days). The regression model used is:

$$\eta = B_0 + B_1P + B_2V + B_3U + \varepsilon \quad (12)$$

The variance explained increased to ~47% and 67% (Table. 3a), when regression performed every two and one month respectively, which indicates that the sea level variability explained improves, when the number of data points is reduced. However, for our model to be successful, the mean sea level variability for two months (~60 day periods) or longer could be considered as known and hence the further analysis is carried out using two month duration. In Fig. 8b and Table. 4 (S.N0.11-14), shows the regression coefficient for independent variables as mentioned in equation-12 at 95% confidence interval along with the lower(upper) confidence bounds LCB(UCB). B_0 (black) varies from -11 to 8 cm, is the mean sea level during the regression duration of two months. The time variability of B_0 is very close to a seasonal cycle (Fig.11). The value for the seasonal sea level cycle in the region is in the range of 8–15 cm (Tsimplis and Woodworth, 1994). Thus it is probably the steric sea level variation of the open ocean that is expressed in this variable. B_1 (blue) is the coefficient corresponding to atmospheric pressure and varies from -2.7 to 0.1 cm/mb, which is a significant deviation from the inverse barometer effects. B_2 (red) is the coefficient corresponding to along shore wind ranging from 0.4 to 6.4 cm/ms⁻¹ and B_3 (green) is the coefficient corresponding to cross shore winds ranging from -7.2 to 3 cm/ms⁻¹. Fig. 8c&d shows the estimated sea level residuals during June-August of 2007 & 2008 with the SLR variability's explained up to 42% & 47% respectively.

Table. 4 is listed with the residual variability explained by different independent variables along with their variance during the period of two months (also see Fig. 9 a&b). It is observed that the along-shore wind (V) alone is able to explain up to 39(42) % of the tidal residual variability during May-June in 2007 (2008) respectively. The cross-shore wind (U) alone is able to explain up to 40(26) % of the residual variability during June-August, 2007(2008) respectively. The atmospheric pressure alone is able to account up to 6.3(65) % of residual variability during May-June, 2007(2008) respectively. The combined output using along-shore, cross-shore and the atmospheric pressure (Fig. 10a) explains up to 47(75) % of the tidal residual variability during May-June, 2007(2008) respectively. During May-June, both U & V shows a fast rise as compared to the fall during July-August as shown in Fig. 10b. In the year 2007, during summer monsoon, U>0 and also V>0, the residual variability explained is 36-47 %. However, in the summer monsoon of 2008, U>0, V>0 during June and U>0, V<0 during July-August, the percentage variability explained by the model is high up to ~72.5% in May-June and falls to a low of 27% during July-August.

The need to use variable coefficients in order to make the regression work indicates that during the summer monsoon, the tidal residuals in Goa are due to local forcing or that the remote and the local atmospheric forcing are coherent. By contrast during winter monsoon the local forcing is of less importance and other factors most likely the steric sea level is important in determining sea level variations.

Conclusions

The sea level variation at Goa, west coast of India has been studied using approximately two years of data. The sea level variability has been compared and statistically modeled by use of various forcing parameters. Wind and surface geostrophic along-shore currents were found to be coherent with the observed sea level variations. The analysis performed indicates that cross-shore wind component (U) remains land-ward ($U>0$), except during winter monsoon ($U<0$), when the currents along the coast of west India returns to northward. However during the period November-January the local wind components are small in magnitude. The alongshore wind component V remains generally southward ($V<0$) during the period of observations. During the summer monsoon, V starts changing direction during May and flows northward with maximum energy $\sim 1.3 \text{ m}^2\text{s}^{-2}$ during June ($V>0$). The intensity of V reduces by August $\sim 0.3 \text{ m}^2\text{s}^{-2}$ for the year 2007-2008 and it returns to flow southward during winter monsoon.

Several statistical models were attempted. The major difficulty was found to be in the modeling of the sea level variability with periods longer than two months (~ 60 days) which appears not to be forced by the various local forcing parameters. The local parameters such as atmospheric pressure, along shore and cross shore winds account for up to 47% of sea level variations for the year 2007-2008. A significant part of the unexplained variance is due to seasonal variations probably the steric cycle in the open sea.

Acknowledgements

This collaboration started while the first author visited the National Oceanography Centre (NOC), Southampton under an Indian Ocean Tsunami Warning System (IOWTS) fellowship-2008-2009. We are all grateful to the International Oceanographic Commission for providing us with the opportunity of working together.

R: Correlation coefficient between sea level residual and various parameters at 95% confidence interval for the monthly mean, N=22

	RES	W	U	V	AP	AT	WT	RH	Dn
RES	1.00								
W	-0.15	1.00							
U	-0.24	0.87	1.00						
V	0.02	0.69	0.52	1.00					
AP	0.12	-0.73	-0.82	-0.69	1.00				
AT	0.07	0.12	0.18	0.14	-0.38	1.00			
WT	0.10	-0.12	-0.09	0.01	-0.11	0.89	1.00		
RH	-0.13	0.63	0.75	0.62	-0.83	0.02	-0.28	1.00	
Dn	0.09	-0.57	-0.64	-0.49	0.68	0.08	0.32	-0.64	1.00
P: Significance of correlation									
RES	1.000								
W	0.505	1.000							
U	0.284	0.000	1.000						
V	0.945	0.000	0.013	1.000					
AP	0.597	0.000	0.000	0.000	1.000				
AT	0.747	0.608	0.422	0.545	0.079	1.000			
WT	0.669	0.584	0.679	0.973	0.632	0.000	1.000		
RH	0.567	0.002	0.000	0.002	0.000	0.933	0.203	1.000	
Dn	0.693	0.006	0.001	0.021	0.001	0.713	0.146	0.001	1.000

Table. 2 The correlation coefficients (R) between the various parameters (monthly-mean for 2007-2008) at 95% confidence interval. P: is a matrix of p-values for testing the hypothesis of no correlation. Each p-value is the probability of getting a correlation as large as the observed value by random chance, when the true correlation is zero. If P(i,j) is small, say less than 0.05, then the correlation R(i,j) is significant.

Note: RES, Sea level residual; W, Wind speed; U, Cross-shore wind; V, Along-shore wind; AP, Atmospheric pressure; AT, Air temperature; WT, Water temperature; RH, relative humidity and Dn, Water density.

Table 3a

Sr. No.	Variable	Var _e	Variable	Var _e	Variable	Var _e
1	Dn	0.05	AP U	0.79	AP V Tdiff	6.69
2	AP	0.09	AP τ_{sy}	5.94	AP V WT	6.75
3	WT	0.01	V Tdiff	6.53	AP U V	7.72
4	Tdiff	0.17	V Dn	6.53	AP τ_{sy} GC	24.69
5	U	0.79	AP V	6.59	U V GC	25.14
6	τ_{sy}	5.85	V WT	6.64	AP U V GC	25.97
7	V	6.46	U V	6.94	AP U V GC Tdiff	25.98
8	GC	14.1	AP GC	20.0	AP U V GC WT	26.21
9			V Gc	22.63	AP U V GC Dn	26.63
10					AP U V (every two months)	47.63
11					AP U V (every one month)	67.3

Table 3b

The coefficient estimates at 95% confidence interval for the independent variables U, V, and GC with $R^2(\text{statistic})=0.26$.			
Coefficient of regression	LCB	Coefficient estimates at 95% confidence interval	UCB
B ₀	0.89	1.03	1.16
B ₁	-0.41	-0.36	-0.30
B ₂	0.45	0.54	0.62
B ₃	2.35	2.49	2.64
B ₄	0.23	0.24	0.24

Table. 3 a Shows the percentage variability for various parameters. The coefficients are estimated at 95% confidence interval. Sr.1-9, the multilinear regression is performed over the period from 1 January 2007 to November 2008. In Sr. 9, the regression analysis is performed over the window of two months. b The coefficient estimates at 95% confidence interval for the independent variables U, V, and GC along with lower (upper) confidence bounds LCB (UCB). Note: AP, Atmospheric pressure; WT, Water temperature; Tdiff, WT-AT; U, Cross-shore wind; V, Along-shore wind; AT, Air temperature; GC, Geostrophic currents; τ_{sy} , surface stress and Dn, water density.

SN	Variables	Total Var _e	Variability explained Var _e (%)										
			2007						2008				
			J-F	M-A	M-J	J-A	S-O	N-D	J-F	M-A	M-J	J-A	S-O
1	V	29.6	10.3	-0.2	39.0	1.7	24.5	1.5	14.2	7.6	42.5	0.6	10.5
2	U	30.1	0.1	1.2	8.0	40.5	8.0	1.3	8.3	19.2	24.0	26.3	22.4
3	AP	29.5	0.9	16.2	6.3	17.0	24.8	7.9	0.9	3.4	65.0	11.2	22.4
4	AP,U	37.6	0.9	17.1	9.7	43.0	24.9	7.9	14.9	26.2	65.2	27.4	31.7
5	AP,V	38.8	11.4	16.2	39.3	18.1	36.7	10.0	16.8	9.1	73.3	11.3	32.6
6	U,V	42.9	12.3	7.0	46.8	40.8	27.6	2.6	18.8	24.2	63.4	26.7	29.0
7	AP,V,U	47.6	12.8	17.8	47.0	43.1	36.7	10.0	27.1	28.6	75.5	27.6	39.3
	R ² (statistic)		0.13	0.19	0.46	0.43	0.37	0.10	0.27	0.29	0.75	0.28	0.39
Variance													
8	V (m ² S ⁻²)		0.22	0.46	1.68	0.55	0.63	0.09	0.31	0.21	1.01	0.11	0.23
9	U (m ² S ⁻²)		0.24	0.17	3.56	4.37	1.01	0.65	0.28	0.13	2.09	1.50	0.64
10	AP (mb ²)		1.77	1.43	7.22	2.18	3.62	1.94	1.47	2.51	2.11	2.71	3.44
Coefficient of regression													
11	UCB		3.2	6.1	-6.7	-10.9	-3.0	2.5	10.3	9.0	-7.0	7.0	0.8
	B ₀ (cm)		2.4	5.4	-7.2	-11.6	-3.3	2.1	8.8	8.5	-7.3	-7.2	0.6
	LCB		1.6	4.8	-7.7	-12.3	-3.7	1.7	7.3	8.1	-7.6	-7.9	0.3
12	UCB		-0.1	-0.8	0.3	-0.8	-1.0	1.0	-2.2	-0.6	-2.6	-0.3	-0.9
	B ₁ (cm/mb)		-0.3	-1.0	0.1	-1.1	-1.2	0.8	-2.7	-0.8	-2.8	-0.5	-1.0
	LCB		-0.5	-1.3	0.0	-1.4	-1.4	0.7	-3.1	-1.0	-3.1	-0.8	-1.1
13	UCB		4.9	0.8	4.3	0.1	3.2	-1.3	7.2	2.6	3.4	0.0	3.5
	B ₂ (cm/ms ⁻¹)		4.3	0.4	4.1	-0.4	2.9	-1.9	6.4	2.1	3.2	-1.1	3.1
	LCB		3.7	0.0	3.8	-0.9	2.6	-2.5	5.6	1.5	2.9	-2.1	2.6
14	UCB		2.0	1.7	1.5	2.4	0.4	0.4	-5.8	-6.5	1.2	3.3	2.2
	B ₃ (cm/ms ⁻¹)		1.4	1.1	1.3	2.2	0.1	0.1	-6.8	-7.2	1.0	3.0	1.9
	LCB		0.9	0.5	1.1	2.0	-0.2	-0.1	-7.7	-7.9	0.9	2.6	1.6

Table 4. Results of estimation of SLR using multilinear regression analysis over a window of two months from January 2007 to October 2008. The estimated coefficients reported are at 95% confidence interval.

S.N. 1 to 7 is listed with sea level variability explained by different independent variables using multivariate regression for duration of two months (months are represented by their first letter, for e.g. J-F means January to February) from January 2007 to October 2008. The sea level residual variability explained by AP, V and U are listed at S.N. 7 along with R² (Statistics). S.N. 8 to 10 is listed with the variance of V, U and AP. S. N.-11 to 14 is listed with the coefficients of regression for Offset, AP, V and U for the respective two month duration at 95% confidence interval along with the lower (upper) confidence bound LCB (UCB).

References

- Banse K (1968) Hydrography of the Arabian Sea Shelf of India and Pakistan and effects on demersal fishes. *Deep-Sea Research* 15, 45–79.
- Bell C, Vassie J M and Woodworth P L (2000) Tidal Analysis Software Kit 2000 (TASK-2000). POL/PSMSL Permanent Service for Mean Sea Level, Proudman Oceanographic Laboratory, UK.
- Csanady G T (1974) Barotropic currents over the Continental Shelf. *J. Phys. Oceanogr.*, 4, 357-371.
- Csanady G T and Scott J T (1974) Baroclinic coastal jets in Lake Ontario during IFYGL. *J. Phys. Oceanogr.*, 4, 524-541.
- Fofonoff N P and Tabata S (1966) Variability of oceanographic conditions between ocean station P and Swiftsure Bank off the Pacific coast of Canada. *J. Fish. Res. Board Can.*, 23,825-869.
- Gill A E and Niiler P P (1973) The theory of the seasonal variability in the ocean. *Deep Sea Res* 20: 141–177.
- Hasternrath S and Lamb P J (1979) Climate atlas of the Indian Ocean. Part I: surface climate and atmospheric circulation. Wisconsin University Press, Madison, 97, 19pp.
- Hsu S A (1974) On the log-linear wind profile and the relationship between shear stress and stability characteristic over the sea. *Boundary Layer Meteorol.*, 6, 509-514.
- Hyun-Sook Kim, Flagg C N and Howden S D (2001) Northern Arabian Sea variability from TOPEX/Poseidon altimetry data: an extension of the US JGOFS/ONR shipboard ADCP study. *Deep-Sea Research*, 48, 1069-1096.
- Joseph A, Vijaykumar, Desa E, Ehrlich D, and Peshwe V (2002) Over-estimation of sea level measurements from water density anomalies within tide-well – A case study at Zuari estuary, Goa. *JCR*, 18,2, pp-362-371.
- Johannessen O M, Subharaju G and Bliondhiem (1981) Seasonal variation of the oceanographic conditions off the southwest coast of India during 1971-75. *FiskDir Skr. Ser. HavUnders.*, 18, 247-261.
- Krishnamurti T N and Bhalme H N (1976) Oscillations of a monsoon system. Part I. Observational aspect. *J. Atmos. Sci.*, 33, 1937–1954.
- Lighthill M J (1969) Dynamic response of the Indian Ocean to the onset of the southwest monsoon. *Philos. Trans. R. Soc. London, Ser. A*, 265, 45– 92.
- Mehra P, Prabhudesai R G, Joseph A, Vijay K, Dabholkar N, Prabudesai S, Nagvekar S and Agarvadekar Y (2005) Endurance and Stability of Some Surface Meteorological Sensors under Land- and Ship-Based Operating Environments. *Proceedings of the*

National Symposium on Ocean Electronics, SYMPOL-2005, 15-16 December 2005, pp. 257-264.

Mehra P, Joseph A, Prabhudesai R G, Vijay K, Sundar D, and Tengali S (2008) On the usability of “compensated temperature” output of Honeywell PPTR sensor for coastal oceanographic and limnological studies. Proceedings of the International Conference: Oceans’08 MTS/IEEE-Kobe-Techno-Ocean’08 (OTO’08) from 8-11 April 2008.

Prabhudesai R G, Joseph A, Agarvadekar Y, Dabholkar N, Mehra P, Gouveia A, Tengali S, Vijay K and PARAB A (2006) Development and implementation of cellular-based real-time reporting and Internet accessible coastal sea level gauge- A vital tool for monitoring storm surge and tsunami. *Current Science*: 90(10);1413-1418.

Prabhudesai R G, Joseph A, Mehra P, Agarvadekar A, Tengali S, and Vijay K (2008) Cellular-based and Internet-enabled real-time reporting of the tsunami at Goa and Kavaratti Island due to *M_w* 8.4 earthquake in Sumatra on 12 September 2007. *Current Science*: 94, 10 May 2008; 1151-1157.

Schott F A and McCreary J P (2001) The monsoon circulation of the Indian Ocean. *Prog. Oceanogr.*, 51, 1 – 120.

Sandstrom H (1980) On the Wind-Induced Sea Level Changes on the Scotian Shelf. *Journal of Geophysical Research*, Vol. 85, 461-468.

Shankar D (2000) Seasonal cycle of sea level and currents along the coast of India. *Current Science*, 78, 279–288.

Shankar D, Vinayachandran P N and Unnikrishnan A S (2002) The monsoon currents in the north Indian Ocean. *JPO* 52 (2002) 63-120.

Shankar D and Shetye S R (1997) On the dynamics of the Lakshadweep high and low in the southeastern Arabian Sea. *Journal of Geophysical Research* 102, 12551–12562.

Shankar D, and Shetye S R (1999) Are interdecadal sea level changes along the Indian coast influenced by variability of monsoon rainfall. *Journal of Geophysical Research* 104, 26031–26042.

Shankar D, and Shetye S R (2001) Why is the mean sea level along the Indian coast higher in the Bay of Bengal than in the Arabian Sea? *Geophysical Research Letters* 28, 563–565.

Shetye S and Shenoi S S C (1988) Seasonal cycle of surface circulation in the coastal North Indian Ocean. *Proceedings of Indian Academy of Sciences (Earth Planetary Science)* 97, 53-62.

Shetye S R, Suresh I, Shankar D, Jayakumar S, Mehra P, Prabhudesai R G and Pednekar P S (2008) Observational evidence for remote forcing of the West India coastal current. *Journal of Geophysical Research*, 113, 10 pp; doi:10.1029/2008JC004874.

Srinivas K, Kesavadas V and Dineshkumar P K (2005a) Statistical modeling of monthly mean sea level at coastal tide gauge stations along the Indian subcontinent. *Indian Journal of Marine Sciences*, 34, 212–224.

Srinivas K, Dineshkumar P K and Revichandran C (2005b) ENSO signature in the sea level along the coastline of the Indian subcontinent. *Indian Journal of Marine Sciences*, 34, 225–236.

Stammer D (1997a) Global characteristics of ocean variability estimated from regional TOPEX/POSEIDON altimeter measurements. *Journal of Physical Oceanography*, 24, 305–325.

Stammer D (1997b) Steric and wind-induced changes TOPEX/POSEIDON large-scale observations. *Journal of Geophysical Research*, 102(9), 20987–21009.

Sundar D and Shetye S R (2005) Tides in the Mandovi and Zuari estuaries, Goa, west coast of India *J. Earth Syst. Sci.* 114, No. 5, October 2005, pp. 493–503.

Tsimplis M N and Woodworth P L (1994) The global distribution of the seasonal sea level cycle calculated from coastal tide gauge data. *Journal of Geophysical Research* 99, 16031–16039.

Weatherly G L (1975) A numerical study of time-dependent turbulent Ekman layers of horizontal and sloping bottoms. *J. Phys. Oceanogr.*, 5, 288–299

Woodworth P L, Aman A and Aarup T (2007) Sea level monitoring in Africa. *AJMS* 29(3), 321–330.

Wyrski K (1971) *Oceanography atlas of the International Ocean Expedition*. U.S. Government Printing Office, Washington, DC, 531pp.

Wyrski K (1973) Physical oceanography of Indian Ocean. In: *The biology of the INDIAN OCEAN*. B. ZEITZSCHEL and S. A. GERLACH, editors, Chapman and Hall, London, pp. 18–36.

Figures

Fig. 1 a The west coast of India along with the satellite Jason track-181. The x marks indicate the nearest and farthest altimeter data point from the coast used in this study. **b** Map of the study region of Goa (adapted from Fig.1, Sundar & shetye, 2005). Sea level was measured at Verem using a pressure and radar tide gauge (15.5°N, 73.80°E). The surface meteorological parameters were measured using an automatic weather station (AWS) located on the terrace of the National Institute of Oceanography in Dona Paula (15.46°N, 73.80°E) at an height of ~48 m with respect to MSL.

Fig. 2 a Comparison between the residuals obtained from the radar and pressure gauge installed at Verem. **b** The difference between the two systems: Difference=Radar gauge-Pressure gauge (cm) The average difference is ~ -2 cm with a standard deviation of 3.2 cm. The thick line shows the 24 hr running average and is confined within ± 5 cm.

Fig. 3 Monthly-mean sea level anomalies. Black dotted line represents Marmugao, the data obtained from PSMSL, station code=500/065; Red plus line show altimetry data from the nearest point to Marmugao along the Jason track, (Lat: 14.0°N, Lon: 73.8°E) and Grey starred line shows data from the farthest point to Marmugao along the Jason track (Lat: 9.0°N, Lon: 72.0°E, also refer Fig.1).

Note: The sea level during winter (summer) monsoon is trough (crest). Also note the sharp change in sea level from October to November when the WICC reverses from southward to northward.

Fig. 4 Hourly measurements of **a** tides; **b** Sea level residual; **c** wind speed; **d** wind direction; **e** Atmosphere pressure; **f** water temperature; **g** Air temperature and **h** relative humidity at Goa, India. SM - Summer monsoon.

Fig. 5 Hourly time series of sea level and surface meteorological data. **a** Sea level residual after removing the astronomical tide; **b** Geostrophic currents 'GC' estimated from the average of the current obtained from the sea level anomaly gradient from 13° N to 14° N along the Jason satellite track-181; **c** U - Cross shore wind; **d** V – Along shore wind; **e** Atmospheric pressure anomaly and **f** Water density. Note: Except GC and water density all

the other parameters are subjected to a convolution filter with Hanning window of 36 data points. SM - Summer monsoon.

Fig. 6 Power spectrum (95% confidence limit) of **a** Sea level residual (SLR) along with the time-period 'T' (in days) indicated near the prominent peaks. **b** spectrum of anomalies of cross-shore & along-shore winds and atmospheric pressure. Note: The data used for spectrum analysis is from 5th May 2007 to 13th November 2008 of hourly samples without the use of filter. The spectrum of data series is obtained using the 'pwelch' function from Matlab over the total number of samples-N=13463 with Hamming window of length-2048 points with 50% overlap.

Fig. 7 Estimation of sea level residuals using multivariate regression with **a** AP, U and V and **b** AP, U and V and geostrophic currents 'GC' as independent variables.

Fig. 8 a Estimation of sea level residuals using multivariate regression for a duration of two months using AP, U, and V as independent parameters. **b** The derived regression coefficients for the 60 day periods. B_0 - offset, B_1 - AP, B_2 - V and B_3 - U. Estimation of sea level obtained from June-August during summer monsoon **c** for the year 2007 and **d** for the year 2008.

Fig. 9 The percentage variability of sea level residual explained by the model (equation-12) for duration of two months from January 2007 to October 2008. **a** Percentage variability explained by the V, U and AP independently. **b** Corresponding normalized variance (each series divided by respective standard deviation) of V, U and AP during the period of regression. SM: Summer monsoon.

Fig. 10 The percentage variability of sea level residual explained by the model (equation-12) for duration of two months from January 2007 to October 2008. **a** AP, U and V used as independent variables and **b** Monthly-mean along-shore (V) and cross shore(U) winds.

Note: +V→ Northward, -V→ Southward, +U→Landward and -U → Seaward.

Fig. 11 Harmonic fit to the coefficient B_0 indicating seasonal variations. Ssa- 0.0821373 and Mm-0.5443747 degrees/hrs appears to be present.

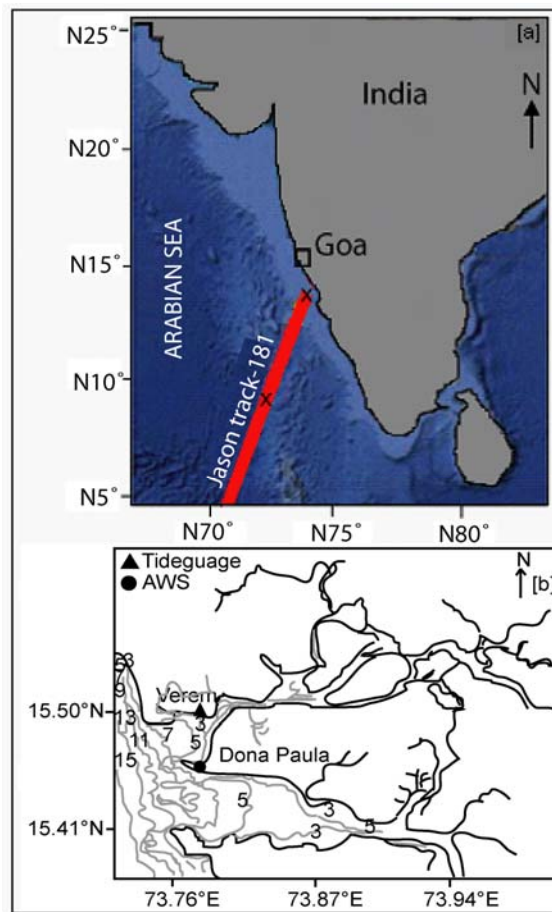


Fig.1

Fig. 1 a The west coast of India along with the satellite Jason tack-181. The x marks indicate the nearest and farthest altimeter data point from the coast used in this study. **b** Map of the study region of Goa (adapted from Fig.1, Sundar & shetye, 2005). Sea level was measured at Verem using a pressure and radar tide gauge (15.5°N, 73.80°E). The surface meteorological parameters were measured using an automatic weather station (AWS) located on the terrace of the National Institute of Oceanography in Dona Paula (15.46°N, 73.80°E) at an height of ~48 m with respect to MSL.

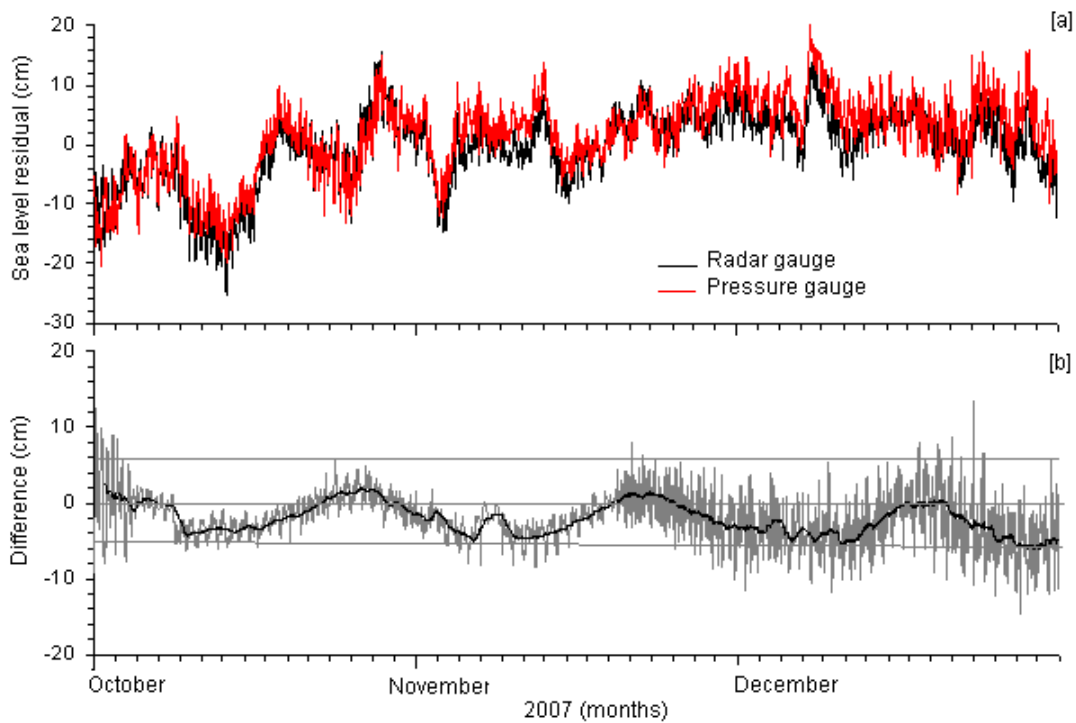


Fig. 2 a Comparison between the residuals obtained from the radar and pressure gauge installed at Verem. **b** The difference between the two systems: $\text{Difference} = \text{Radar gauge} - \text{Pressure gauge}$ (cm) The average difference is ~ -2 cm with a standard deviation of 3.2 cm. The thick line shows the 24 hr running average and is confined within ± 5 cm.

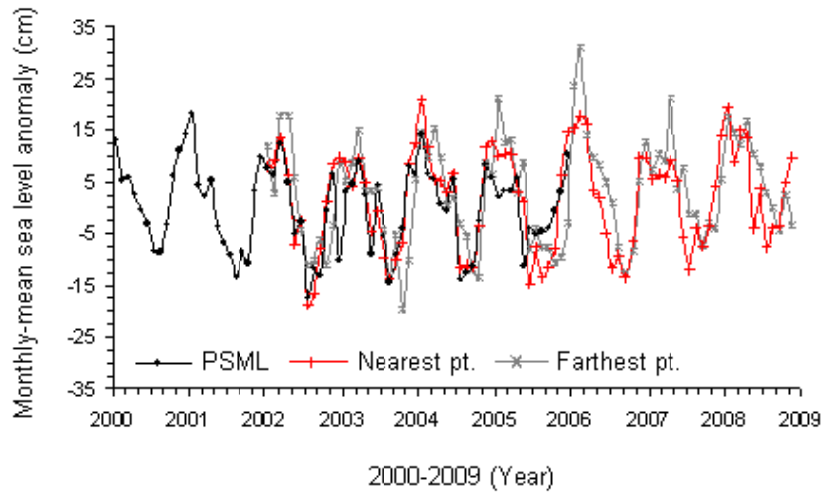


Fig. 3 Monthly-mean sea level anomalies. Black dotted line represents Marmugao, the data obtained from PSMSL, station code=500/065; Red plus line show altimetry data from the nearest point to Marmugao along the Jason track, (Lat: 14.0°N, Lon: 73.8°E) and Grey starred line shows data from the farthest point to Marmugao along the Jason track (Lat: 9.0°N, Lon: 72.0°E, also refer Fig.1).

Note: The sea level during winter (summer) monsoon is trough (crest). Also note the sharp change in sea level from October to November when the WICC reverses from southward to northward.

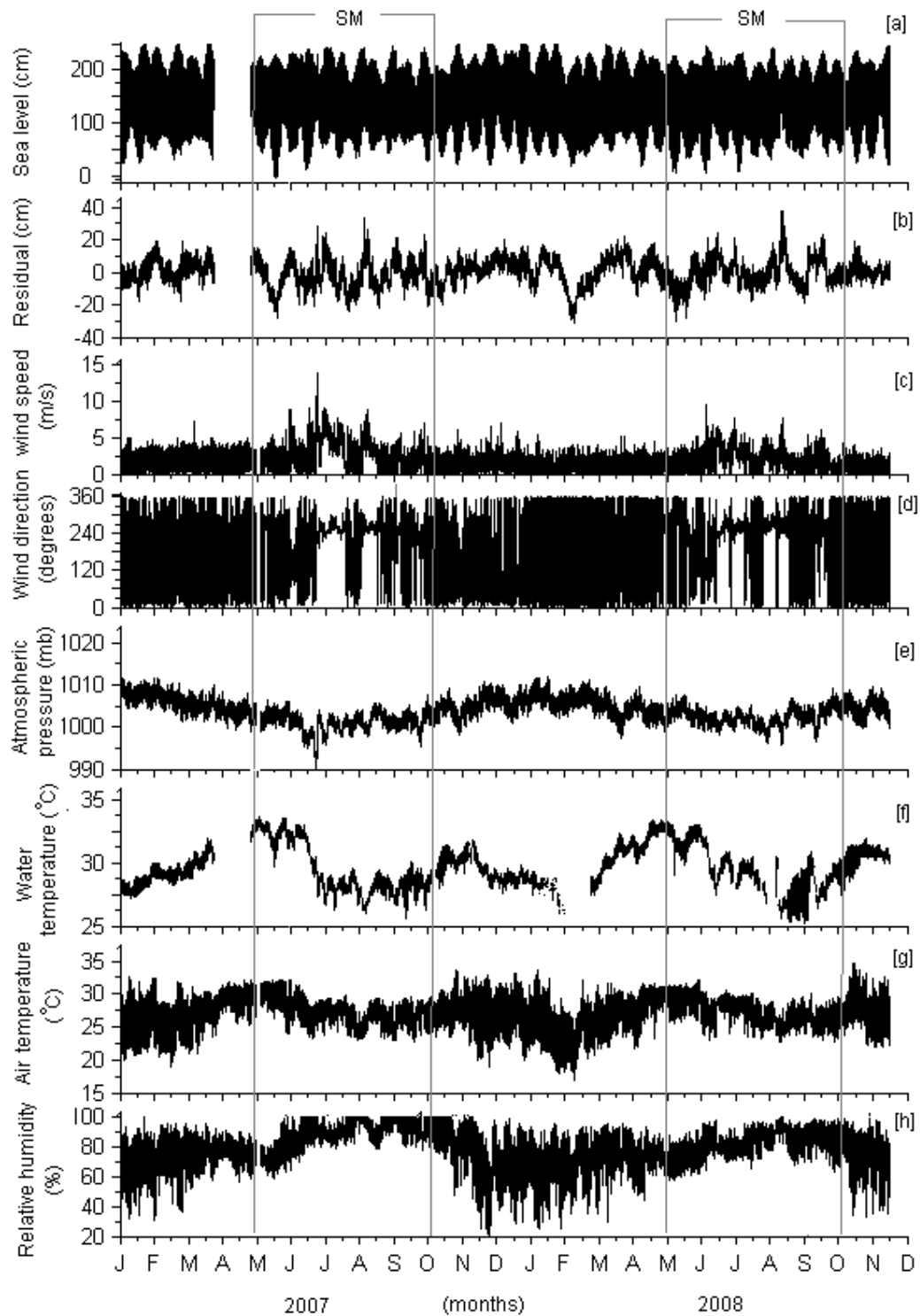


Fig. 4 Hourly measurements of **a** tides; **b** Sea level residual; **c** wind speed; **d** wind direction; **e** Atmosphere pressure; **f** water temperature; **g** Air temperature and **h** relative humidity at Goa, India. SM - Summer monsoon.

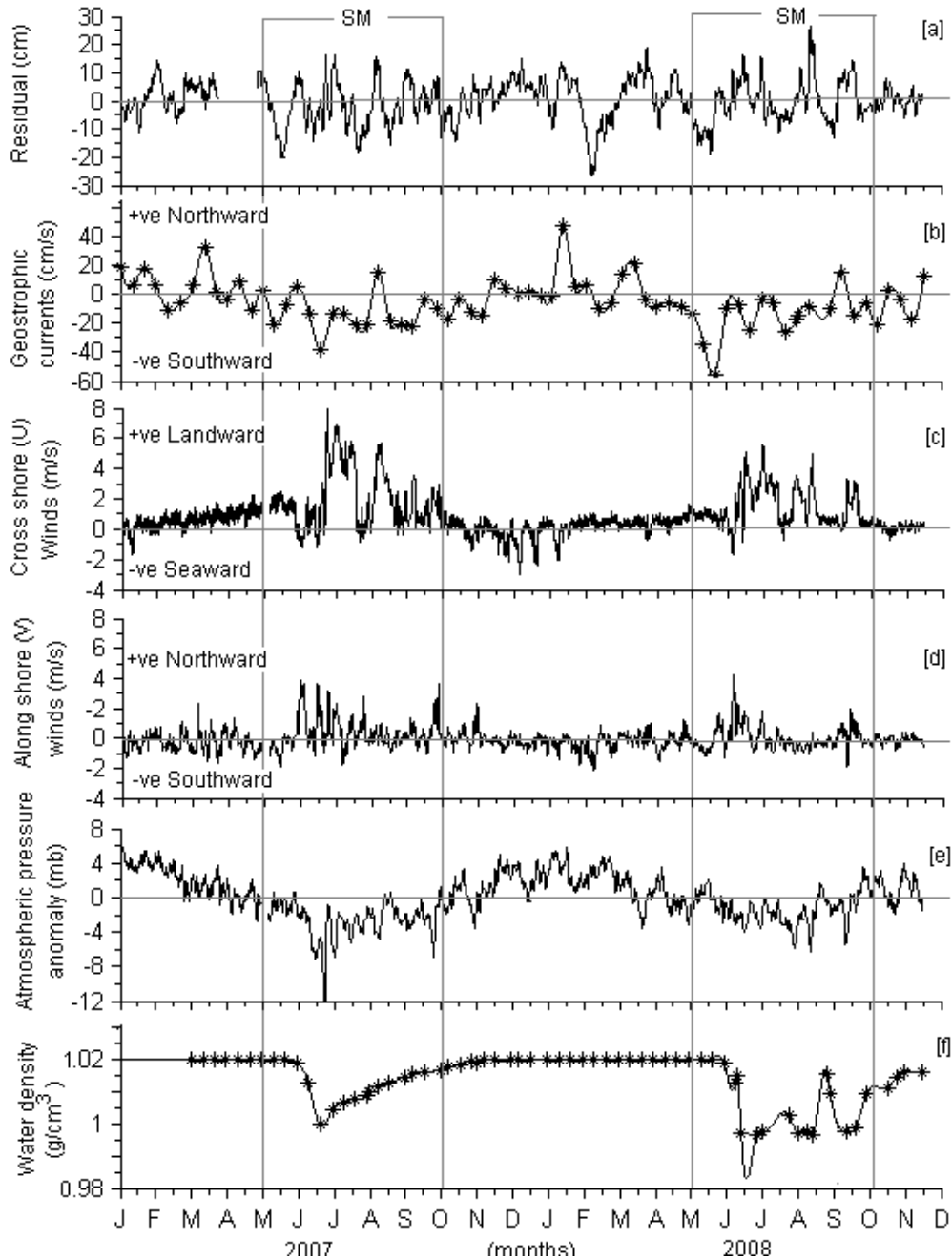


Fig. 5 Hourly time series of sea level and surface meteorological data. **a** Sea level residual after removing the astronomical tide; **b** Geostrophic currents 'GC' estimated from the average of the current obtained from the sea level anomaly gradient from 13° N to 14° N along the Jason satellite track-181; **c** U - Cross shore wind; **d** V – Along shore wind; **e** Atmospheric pressure anomaly and **f** Water density. Note: Except GC and water density all the other parameters are subjected to a convolution filter with Hanning window of 36 data points. SM - Summer monsoon.

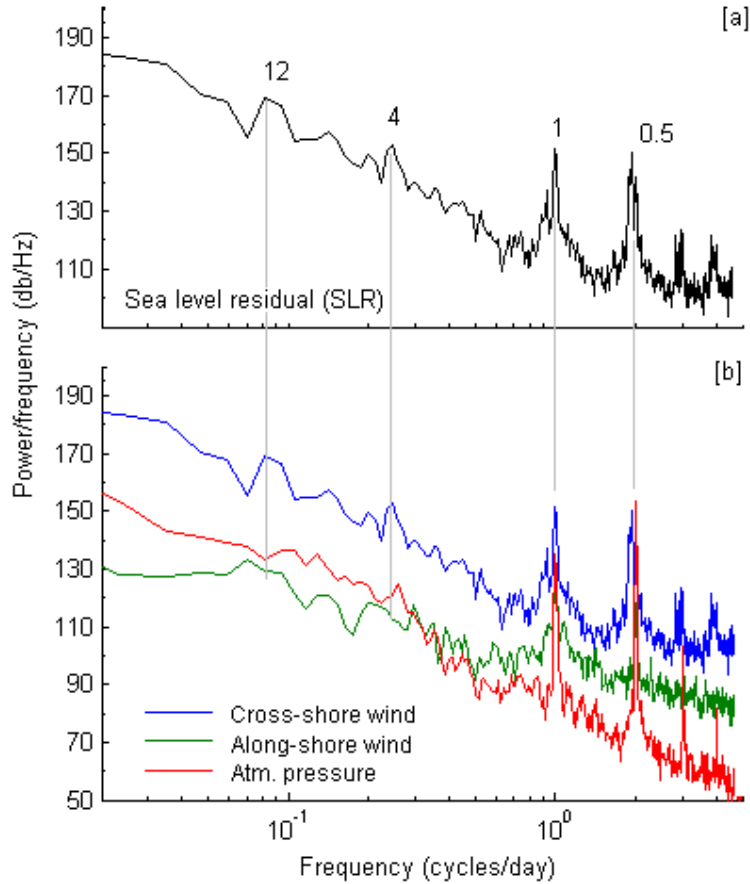


Fig. 6 Power spectrum (95% confidence limit) of **a** Sea level residual (SLR) along with the time-period 'T' (in days) indicated near the prominent peaks. **b** spectrum of anomalies of cross-shore & along-shore winds and atmospheric pressure. Note: The data used for spectrum analysis is from 5th May 2007 to 13th November 2008 of hourly samples without the use of filter. The spectrum of data series is obtained using the 'pwelch' function from Matlab over the total number of samples-N=13463 with Hamming window of length-2048 points with 50% overlap.

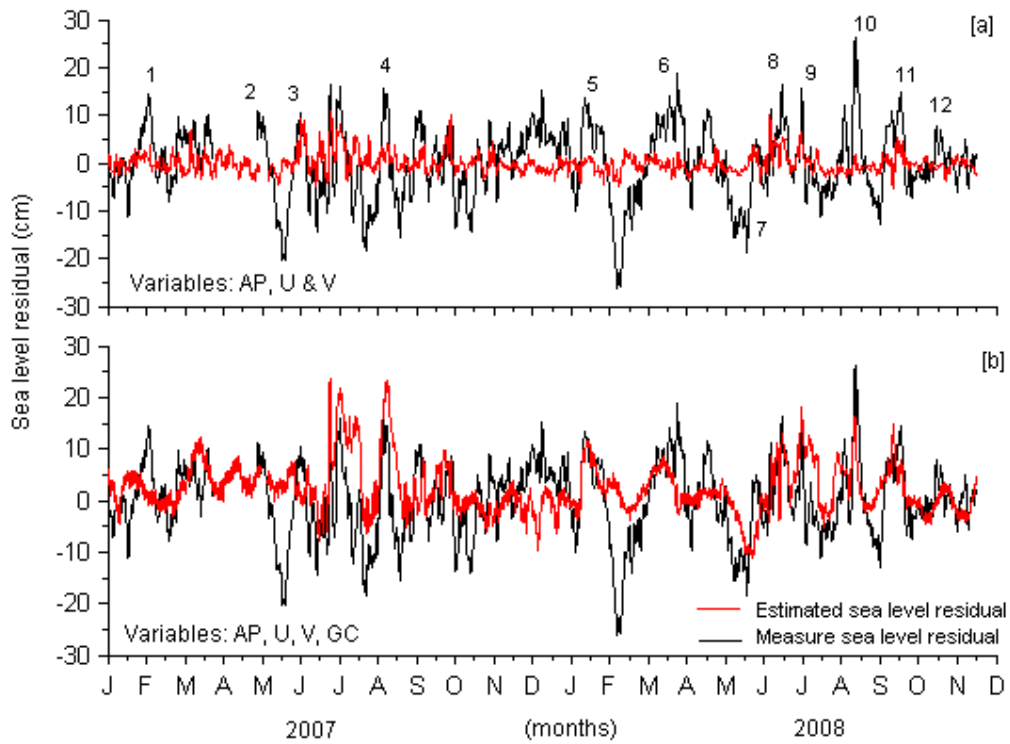


Fig. 7 Estimation of sea level residuals using multivariate regression with **a** AP, U and V and **b** AP, U and V and geostrophic currents 'GC' as independent variables.

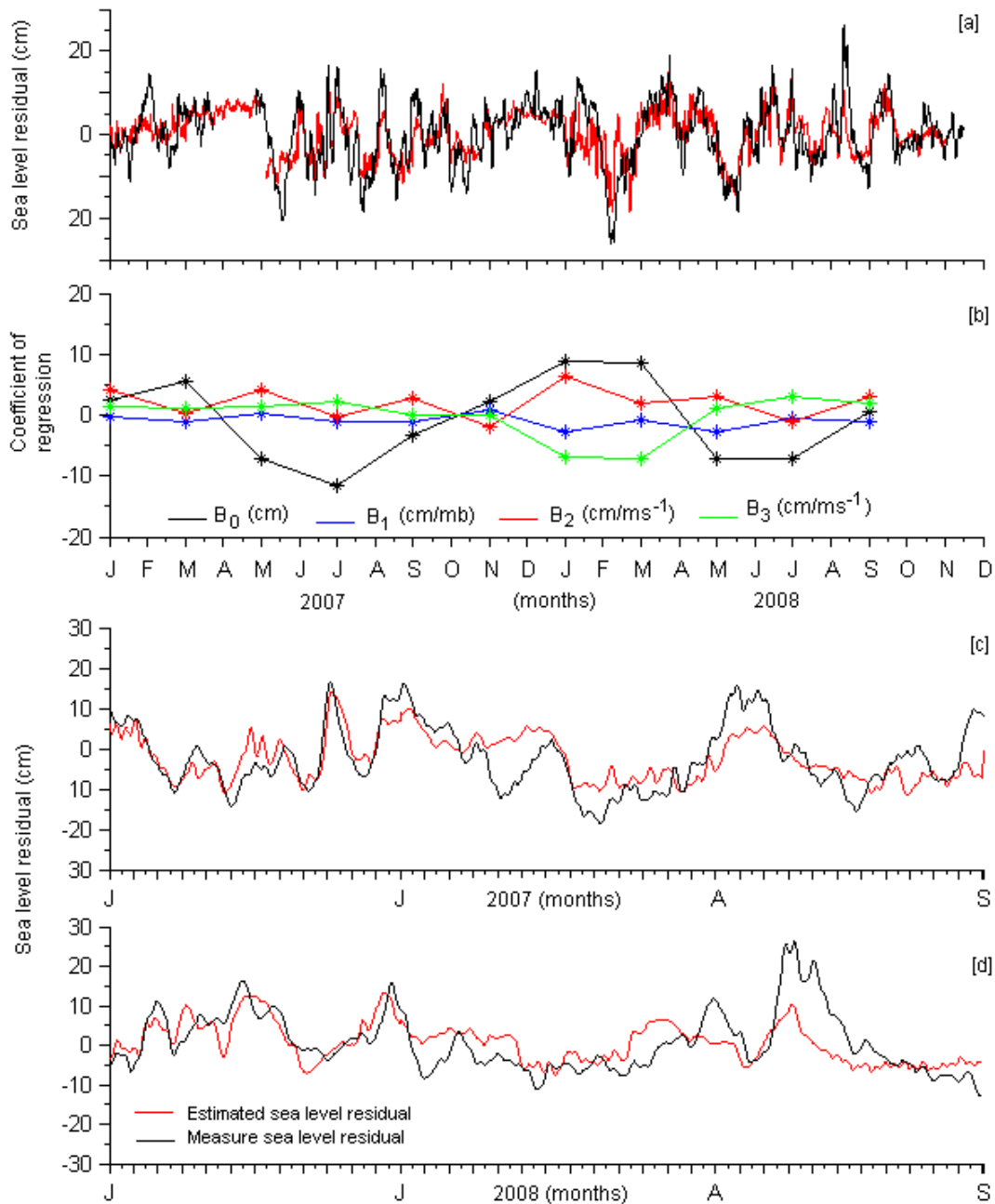


Fig. 8 **a** Estimation of sea level residuals using multivariate regression for a duration of two months using AP, U, and V as independent parameters. **b** The derived regression coefficients for the 60 day periods. B_0 - offset, B_1 - AP, B_2 - V and B_3 - U. Estimation of sea level obtained from June-August during summer monsoon **c** for the year 2007 and **d** for the year 2008.

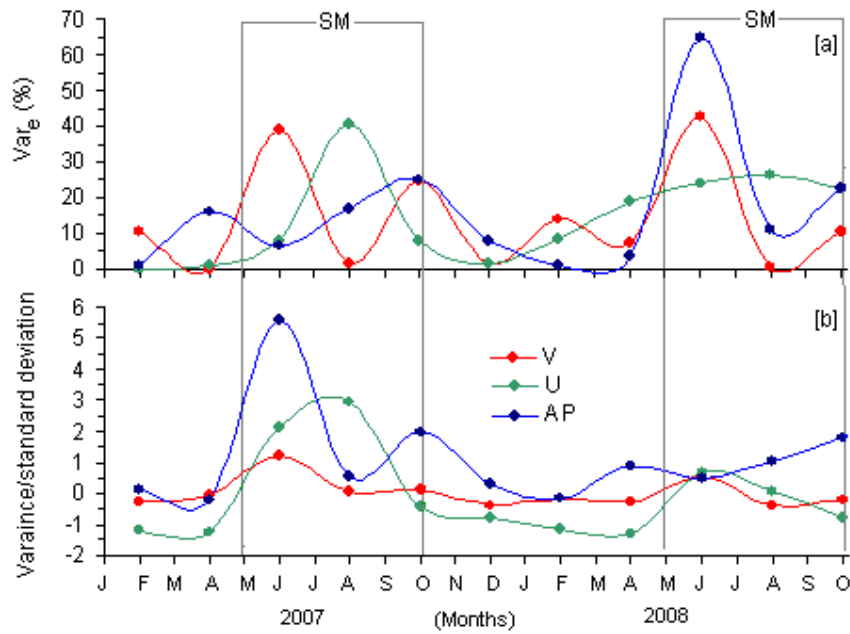


Fig. 9 The percentage variability of sea level residual explained by the model (equation-12) for duration of two months form January 2007 to October 2008. **a** Percentage variability explained by the V, U and AP independently. **b** Corresponding normalized variance (each series divided by respective standard deviation) of V, U and AP during the period of regression. SM: Summer monsoon.

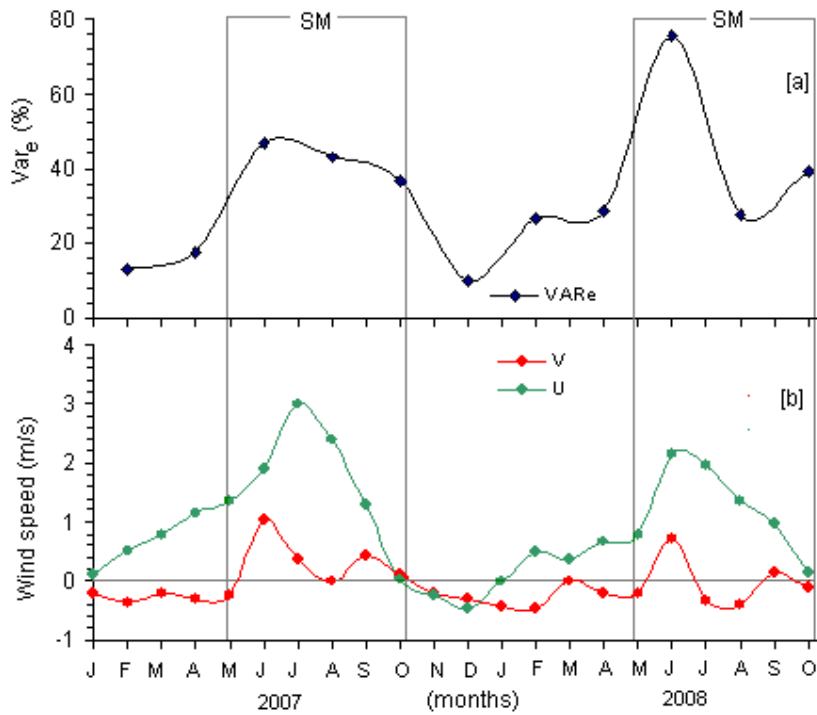


Fig. 10 The percentage variability of sea level residual explained by the model (equation-12) for duration of two months from January 2007 to October 2008. **a** AP, U and V used as independent variables and **b** Monthly-mean along-shore (V) and cross shore(U) winds.

Note: +V → Northward, -V → Southward, +U → Landward and -U → Seaward.

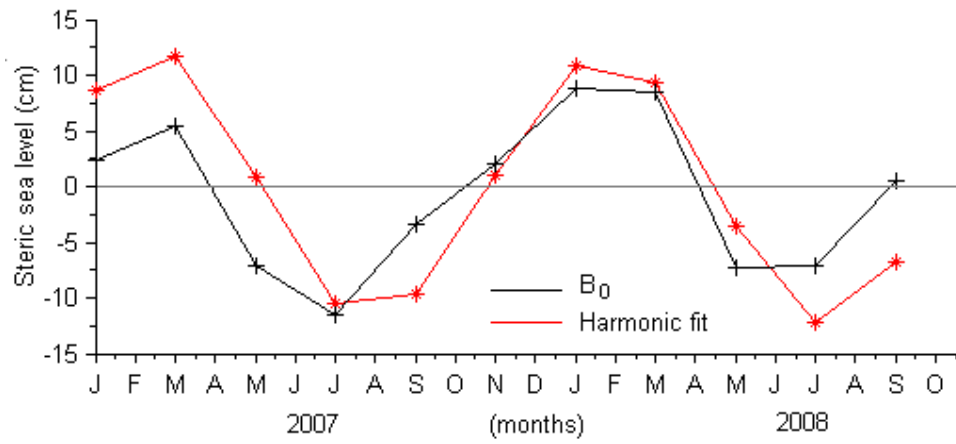


Fig. 11 Harmonic fit to the coefficient B_0 indicating seasonal variations. $S_{sa} = 0.0821373$ and $M_m = 0.5443747$ degrees/hrs appears to be present.